Green Synthesis: CdS Nanoparticle and Dielectric Properties of CdS-PPY Nanocomposite

Kousik Dutta
Assistant Professor in Physics
Department of Physics, Behala College, Parnashree, Kolkata- 700060, INDIA.
E-mail: duttakousik2003@yahoo.co.in

Received May 11, 2017 Accepted June 12, 2017

ABSTRACT *The green synthesis of cadmium sulfide (CdS) nanoparticles has been regarded as the most promising technique for their prospective applications in various system. The synthesis of semiconductor nanoparticles is a growing research area due to the prospective applications for the development of novel technologies. In this paper it is reported that the biosynthesis of Cadmium sulfide nanoparticles (CdS-NPs) by reduction of cadmium sulphate solution, using Aloe Vera leaf exact. Inorganic-organic hybrid nanocomposites are synthesized by dispersing nanosized CdS in the conducting polypyrrole matrix. The morphology of crystalline phase of nanocomposite was determined from Scanning Electron Microscopy (SEM), transmission electron microscopes (TEM) and X-ray diffraction (XRD) spectra. The average size of CdS nanoparticles was in the range of 15 nm and the observed morphology was spherical. The UV-VIS Studies shows that the wavelength of optical absorption peak of CdS nanoparticle increases from 430 nm to 470 nm with the decrease of polypyrrole concentration. Complex impedance and dielectric permittivity of Cadmium sulphide-conducting polypyrrole(PPY) nanocomposite have been investigated as a function of frequency and temperature at different compositions. The dielectric permittivity 3700 is observed. Large value of permittivity is well described by Maxwell-Wagner polarization. Broad and asymmetric dielectric spectra are analyzed by Harviliak - Nigami relaxation function.*

Key Words: *Green Synthesis, CdS nanoparticles, CdS-PPY nanocomposites, dielectric properties.*

I. INTRODUCTION:

Research on nanomaterials has enormously increased during the past years. The intense investigations are motivated by several envisaged application areas for the new class of materials. Novel optical, electrical, and mechanical properties of devices comprising nanocrystalline semiconductors and oxides have been demonstrated in photovoltaic solar cells, light-emitting diodes, and ceramics, sensors, antibacterial studies. Nanoparticles have attracted great interest due to their unique physical and chemical properties, which are different from those of either the bulk material or single atoms. [1] Both equilibrium and dynamic properties of nanomaterials can be vary different from those of their corresponding bulk material or isolated atoms and molecules. [2] Nanoparticles show completely improved properties based on specific characteristics such as size, distribution and morphology. Semiconductor nanoparticles also have crucial role due to size dependent optical, luminescence and electrical properties and have several applications in many research areas. Nanostructure sulfides have been studied extensively with a view to establish a relationship among size, structure and optical properties. [3]

Among these, cadmium sulfide is traditionally known as yellow pigment called 'aurora yellow' has been expansively considered due to its budding technological applications in field effect transistors, solar cells, photovoltaic, light emitting diodes, photo catalysis, photoluminescence, infrared photo detector, environmental sensors and biological sensors [4 -5]. CdS is naturally an n type material with an optical band gap of 2.4 eV. [6] Currently, many workers have focused on cadmium sulphide because of several important properties [7- 8] CdS nanoparticle shows size dependent properties due to its very high surface to volume ratio and quantum confinement at nanoscale. Because of its various applications and properties in plants and plant products are now being used for its large-scale production. Because of these interesting possibilities, there have been some efforts to prepare nanoparticles of CdS. Some researchers focused on the synthesis of CdS nanoparticles by cadmium nitrate and sodium sulfide by coprecipitation method. The capping agents used for CdS nanoparticle synthesis like mercaptoaccetate, thiourea etc., have their own demerits like toxic nature, tedious workup, cost and hazard to the environment. [9] Green Chemistry

principles are widely used in Nanosciences recent years. Simple, green and novel method of nanoparticle synthesis is now a great area of interest.

The preparation of CdS nanoparticle has been carried out using various methods, such as polymer template-guided synthesis[10] hydrothermal and solvothermal methods[11-12] Sol-gel, [13] micelss, [14] chemical, biological methods, evaporation, spray pyrolysis, sputtering, chemical method metal organic chemical vapor deposition (MOCVD) and green method. To control the growth of the nanoparticles organic stabilizer (polymer) e.g polyethylene oxide(PEO) poly N- Vinyl 2 pyrolidone (PVP) polyvinylenabazle (PVK) are added during the wet chemical synthesis for capping the surface of the particle. The synthesis of nanoparticle different methods, including using biological methods as capping agents, has been pursued.

Among these methods, green method is considered to be the most suitable method due to its ease of formation, simplicity, inexpensive, ecofriendly and nonpolluting. In addition, the nanoparticles obtained using plant extracts have different shapes and sizes in contrast with those produced by other methods. The advantages of using plant and plant-derived materials for biosynthesis of metal nanoparticles have attracted researchers to investigate mechanisms of metal ions uptake and bio-reduction by plants, and to understand the possible mechanism of metal nanoparticle formation in plants. CdS nanoparticles are prepared by various cadmium source precursors such as cadmium nitrate, cadmium acetate, cadmium chloride, cadmium oleate and cadmium sulphate. Present work reports the green synthesis of CdS NPs using alovera plant extract having ecofriendly polyphenols which acts as a reducing agent and a capping agent, using cadmium sulphate precursor.

The shape plays an important role in determining the electronic properties of nanomaterials. CdS nanocrystals which are prepared using green synthesis technique are dispersed in the polymer matrix to design hybrid nanocomposites. Conducting polymers are very useful supporting medium for the electrical characterisations of nanostructured systems. Polyporrole (PPY) is one of the most studied conducting polymer because of its good electrical conductivity, environmental stability and relative easy synthesis. [15] Conducting polymer are founding a growing number of application in various electronic devices such as in chemical sensors, light emitting diodes, electrochromic display devices etc. among these polymer polyaniline and polypyrrole has been studied most extensively in recent years due to following reasons: (i) these can be synthesized easily (ii) these are comparatively stable in air (iii) these are relatively cheaper and (iv) these shows number of interesting properties such as chemical sensitivity etc. [16]

Conducting polymer composites (CPC) have drawn considerable interest in recent years because of their electrical and electronic devices. In most of these applications the main objectives are to obtain a sufficient level of conductivity in the material. Lately, it has been found that these composites can exhibits some novel properties such as positive temperature co-efficient (PTC) of resistance, photosensitivity etc. [17–19]

Recently the physical properties of nanomaterials are extensively investigated for potential technological application and to understand the nanoscience. Nanomaterials have two distinct microstructures (i) nonocrystalline grain and (ii) surface and interface (grain boundary) components. The large number of surface and interfaces affect drastically the physical properties of materials. Semiconducting nanomaterials exhibit a very high resistance due to interface effect. Impedance spectroscopy is a powerful tool to distinguish the grain and grain boundary effects in complex system. In this work it is investigated that the electrical and dielectric properties of nanosized CdS in the presence of PPY. Measurement of ac conductivity have been extensively used to understands the conduction process various models such as quantum mechanical tunneling model (QMT) small polaron tunneling model (SPTM), large polaron tunneling model (LPTM) atomic hopping model and the correlated barrier hopping model (CBH) have been proposed to explain the ac conduction mechanism for different materials. In the present work, dispersion of nanosized CdS have been prepared in the presence of conducting Polypyrrole (PPY). Then observe the temperature and frequency dependence of ac conduction and dielectric properties for CdS-PPY nanocomposite.

II. MATERIALS AND METHODS

All the chemicals were of analytical grade and purchased from Merck (India) and used without further purification. Pyrrole (AR grade) was purified and stored at -15^{0}C in a refrigerator prior to use. APS oxidant was used as received and de-ionized water was employed for preparing all the solutions and reagents. The samples were characterized by x-ray powder diffraction patterns employing a scanning rate of 0.02 0 per 2 sec in 2θ range from 20 to 70 using a Philips (PW1710) x-ray diffractometer equipped with monochromatized Cukα radiations. The nanocrystalline powder was pressed inside the sample holder and X-ray data were collected in step scan mode. Morphological studies were performed with JEOL JSM6700F Scanning electron microscope (SEM). Transmission electron micrograph (TEM) was taken from JEOL, JEM 2010 with acceleration voltage of 200 KV. FTIR spectrometer were recorded as Kerr disc on PerkinElmer Spectrum-2000, FTIR spectrophotometer between 500 and 4000 cm^{-1}. UV-visible spectra of the diluted nanocomposite dispersions in the 200-1000 nm range was obtained using Perkins-Elmer instrument. The temperature dependent capacitance (C) and dielectric loss factor (D) were measured by Agilent 4192 Impedance Analyzer. The electrical contacts were made by silver paint on both sides of the sample. Dry powdered sample were made into pellets using a steel die of 1 cm diameter in a hydraulic press under a pressure of 7 ton. The thickness of the samples varies from 0.05 cm to 0.10 cm. For electrical measurements the electrical contacts were made by silver paint.

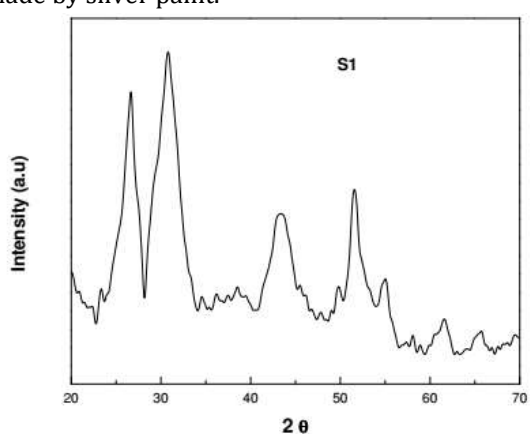

FIG. 1: X-ray diffraction pattern of CdS-PPY nanocomposites sample S1

A. Preparation of aloe Vera leaf extract

Fresh leaves of aloe vera plant were washed with double distilled water and then sun dried for 45 min to remove moisture. 40 g of washed, dried, fine cut leaves were added to 100 mL of deionized water and boiled at 80^0 C for 2 hours until the color of the aqueous solution changes from watery to light yellow.

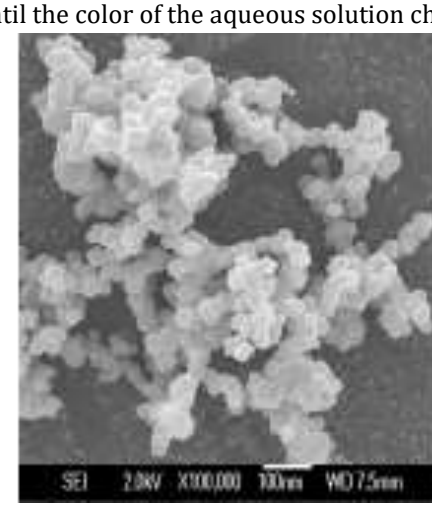

FIG. 2: Scanning Electron Micrograph (SEM) of nanocomposite sample S1.

B. Synthesis of Cadmium sulphide (CdS) nanoparticles by aloe vera leaf extract:

CdS nanoparticles production was done by biosynthesis using aloe vera plant leaf extract as stabilizing/capping agent. For this, 3.5 g of cadmium sulphate (Merck) was added to aloe vera leaf exact solution then boiled it for two and half hours until it changed to a yellow colored paste and is cooled to room temperature. The yellow powder was then collected in a ceramic crucible and calcinated at 600^0 C for 3 hours. A yellow colored powder was obtained and this was carefully collected and dried in a vacuum oven for 60ºC for 2 hours.

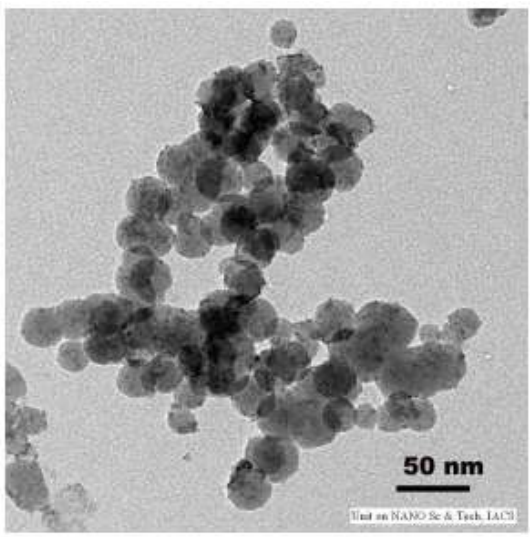

FIG. 3: Transmission Electron Micrograph (TEM) of nanocomposite sample S1.

II. Synthesis of CdS-PPY nanocomposite

The required quantity of CdS nanoparticle was ultrasonically dispersed in 40 ml deionized water. Pyrrole monomer of known volume was slowly added into the dispersion under sonication at room temperature. Then the aqueous solution of APS maintaining a pyrrole : APS mole ratio of 1:1.25 was added drop wise into the previous solution. After few hours the resulting solution was turned into black color which indicates the formation of polypyrrole. The solution was then kept under sonication for about 8 hours to ensure complete polymerization. Finally the resulting black dispersion were centrifuged. The resulting nanocomposites were washed thoroughly with distilled water for several times. Different compositions of nanocomposite samples by varying the weight percentage of pyrrole(polypyrrole) were prepared as shown in Table I.

III. RESULTS AND DISCUSSION:

To confirm the formation of CdS nanoparticles and its crystallographic phase, a wide angle diffractogram (XRD) was recorded for the dried precipitate of CdS nanoparticles. It can be attributed to a very small grain size of the particles. Figure 1 displays the powder X-ray diffraction (XRD) of the sample S1. The characteristic peaks at angles (2θ) of 26.5, 30.8, 43.7, 51.9, 54.9 are indexed to the reflections from 111, 200, 220, 311 and 222 planes of nanocrystalline CdS. It is well known that CdS exists in two crystalline phases, cubic zinc blende and hexagonal wurtzite. The present XRD pattern matches well with the reported cubic phase of CdS [Joint Committee on Powder Diffraction Standards (JCPDS) No. 42-1411]. The peaks are fairly broad suggesting the nanostructure of CdS.

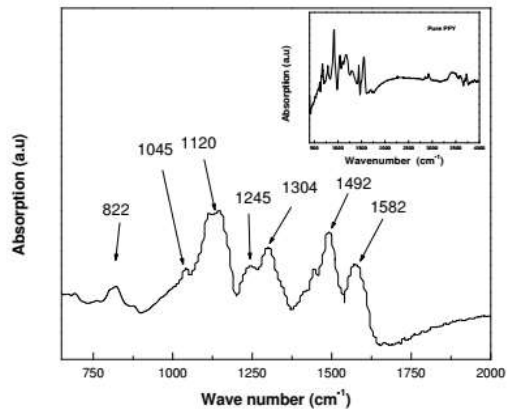

FIG. 4: Fourier Transform Infrared (FTIR) spectra of sample S1 and pure PPY (inset)

The scanning electron micrograph (SEM) of the nanocomposite sample S1 is shown in Figure 2. The CdS nanoparticles are well dispersed and are of spherical in shape with uniform diameter lying in the range from 25- 30 nm. Larger particle size may be due to the aggregation of smaller particles in the presence of polymer matrix.

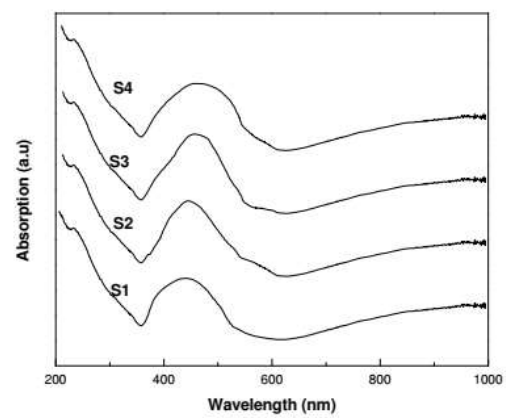

FIG. 5: UV-VIS absorption spectra of the various nanocomposite samples.

Figure 3. shows the TEM micrograph of the CdS polypyrrole nanocomposite S1 sample. In this micrograph nearly, spherical crystallites are observed. The mean particle size of pure CdS is in the range of 12-15 nm which is good agreement with XRD result (Not shown in this manuscripts). Larger particle size due to the aggregation of smaller particles in the presence of polymer matrix having particle size in the range 25-30 nm.

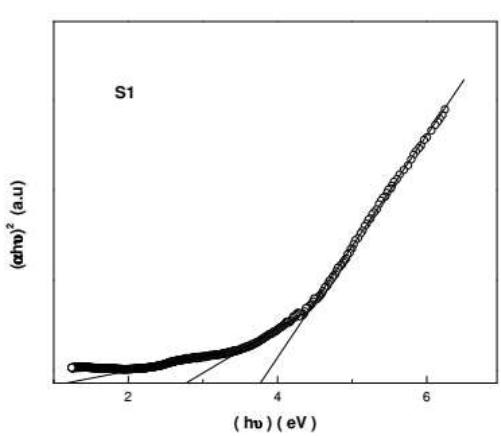

FIG. 6: Plot of (α h ν)² vs. hν for nanocomposite sampleS1 to determine the optical band gap for sample S1.

A typical FTIR spectrum of the nanocomposite sample S1 and pure PPY (Inset) is illustrated in Figure 4. It is to be noted that the absorption peak at 3427 cm^{-1} in the figure is assigned to water molecule. The band at 1582 cm^{-1} corresponds to typical pyrrole rings vibration. The peak at 1492 cm^{-1} is attributed to = CH in plane vibration and peaks at 922 cm^{-1} and 822 cm^{-1} due to = CH out of plane vibration. The characteristic bands at 1304 cm^{-1}, 1245 cm^{-1}, 1045 cm^{-1} are related to C-H and N-H in-plane and bending vibrations. The characteristics bands of bare PPY are 1551 cm^{-1}, 1440 cm^{-1}, 921 cm^{-1}, 788 cm^{-1}, corresponding to pyrrole rings, in and out of plane = CH vibrations. Almost all the bands reveal blue shift in the nanocomposites which indicates that there is a strong interaction between polypyrrole and CdS nanoparticles.

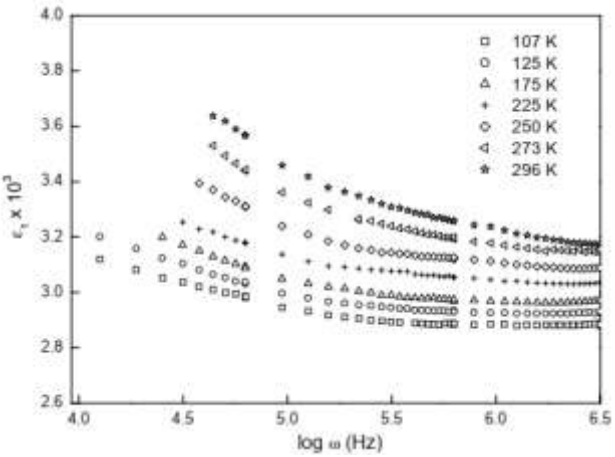

FIG. 7: Real part of the dielectric constant vs. frequency at different temperatures of the sample S1.

Electronic UV-Vis absorption spectra of nanocomposites samples with the variation of polymer fraction are shown in the Figure 5. The fundamental absorption which corresponds to the transition from valance band to the conduction band, can be determine the band gap of the material. The absorption spectra consist of three absorption bands in the entire wavelength range. Out of these three absorption peaks, one prominent broad peak is observed around 430- 470 nm and two broad peaks at 400-1000 nm. Different spectroscopic techniques [20] and theoretical energy band calculation [21] indicate that the absorption band at 400- 500 nm is assigned to π - π^* transition of polypyrrole. Upon doping PPY exhibits an unusual electronic structure due to electron-phonon coupling. Polaron and bipolarons states appear within the band gap which give rise to the broad band at wavelength 600 - 1000 nm The absorption peaks of PPY in the nanocomposites are less pronounced as the strong absorption of CdS overlaps with that of PPY. The absorption peak associated with CdS are found in the wavelength range 470-430 nm. The excitonic peaks for all the samples are well shifted from absorption peak at 530 nm for bulk CdS. The reduction of size in semiconductor reveals a blue shift due to quantum size effect. The dramatic modifications of electronic absorption bands of individual CdS and PPY suggest that nanosized CdS are incorporated into polypyrrole matrix.

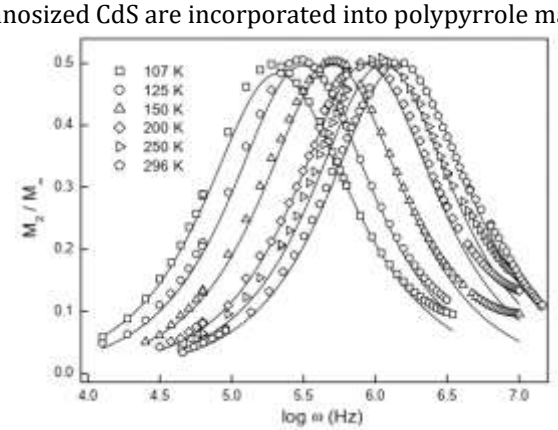

FIG. 8: Imaginary part of electric modulus vs. frequency plot of the sample S1. The solid lines are fit to Eq. 3.

CdS is n-type direct band gap (2.42 eV) semiconductor. Electronic energy band structures of cubic and hexagonal phases of CdS are very similar. [22] 4d states of Cd and 3p states of S play crucial role in the determination of optical band gap. Photoemission experimental results of nanostructured CdS provided the distinct changes of d and p states. [23-24] The optical band gap Eg is related to the absorption coefficient α by the relation [25]

$$\alpha = \frac{B(h\nu - E_g)^{1/2}}{h\nu} \quad (1)$$

where B is the absorption constant for a direct transition. For allowed direct transition one can plot $(\alpha h\nu)^2$ vs. hν and extrapolate the linear portion of it to α = 0 value to obtain the corresponding band gap. The plots of $(\alpha h\nu)^2$ vs. hν for S1 sample is presented in Figure 6. The calculated band gaps are 2.61 eV, 2.69 eV, 2.75 eV and 2.82 eV for S4, S3, S2 and S1 respectively. The higher band gaps compared to the bulk energy gap (2.42 eV) are consistent with the quantum confinement effects of CdS nanoparticles.

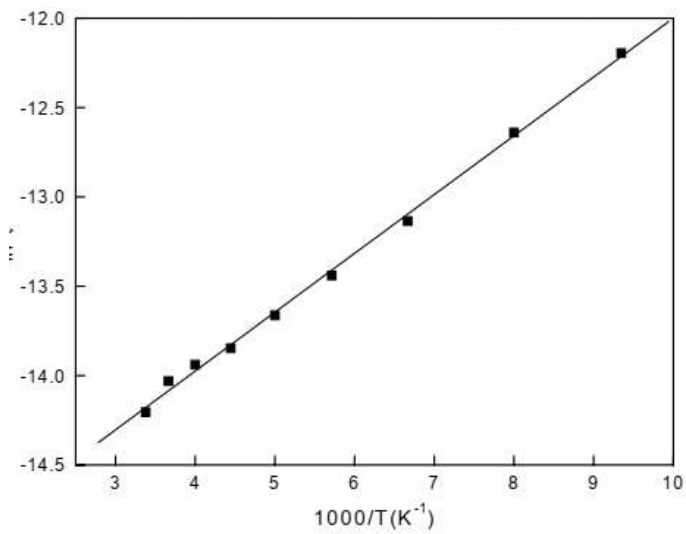

FIG. 9: Arrhenius plot of dielectric relaxation time vs frequency at different temperatures for the sample S1

The frequency dependent dielectric permittivity of a solid arises due to different reasons some of them are as follows (1) displacement of ionic charge with respect to their nuclei in the material (2) displacement of ions from their equilibrium positions and (3) dipolar contribution. Out of these three main contributions only dipolar contribution shows the frequency and temperature dependence at low temperature. Capacitance and dissipation factor were measured within a frequency range 20 Hz to 10 MHz and in the temperature region in between 77 K to 296 K. Real part of complex dielectric function (ϵ1) was determined by considering the geometry of parallel plate capacitor formed by silver paint, the real and imaginary part of the dielectric constant can be calculated from the relation $\epsilon_1 = Cd/A\epsilon_0$. d is thickness and A is area of sample and ϵ_0 is the vacuum dielectric constant. The imaginary component of dielectric constant, ϵ_2 was obtained from $\epsilon_2 = \epsilon_1 D$. Complex impedance Z was calculated from the relation, $Z = 1/(i\omega C_0\epsilon)$, where $C_0 = \epsilon_0 A/d$ is the geometrical capacitance and ω is angular frequency. The dielectric constant ϵ_1 as a function of frequency for different temperature are presented for S1 sample in Fig.7. The magnitude and frequency dependence of ϵ_1 are strongly dependent on the nanosized CdS content. It is observed fact from the figure 7 that the variation of the real part of dielectric permittivity with frequency at constant different temperature that the dielectric permittivity is strongly dependent on frequency at lower frequency region, where ϵ_1 decreases with increasing frequency and the variation is enhanced at higher temperature than the lower temperature. However, a nearly frequency independent behavior has been observed at higher frequency > 1 MHz. This is because, the dipoles at lower temperature are freeze and the polarization decayed for this reason a sharp decrease in ϵ1 has been observed at lower frequency. This type of behavior has been

observed in those samples which have different permittivity and conductivity region. The dielectric permittivity of such an inhomogeneous system can be analyzed by Maxwell-Wagner capacitor model [26–28]. An exceptionally high value of about 3700 is found for the sample with highest content of CdS. In case of more conducting sample S4, ϵ_1 reduces to about 3100.

The frequency dependence of dielectric constant ϵ_1 at several temperatures are presented in Fig. 7. The interesting fact is that a very high dielectric constant of about 3700 at room temperature is found. The maximum value [**29-30**] of dielectric constant (ϵ_1) in CdS is about 8.9 and that of PPY [**31**] is 3.2 at 1000 Hz. The present observation of ϵ_1 is remarkable as it is larger than the constituent materials. The values of ϵ1 remain dispersion less over wide range of frequency. The real part of dielectric constant ϵ_1 does not exhibit a sharp decrease with increase of frequency. The values of dielectric constant as a function of Pyrrole content at the lowest measurable frequencies and at room temperature are shown in Table I. The incorporation of CdS nanoparticles increases the magnitude of ϵ_1 significantly compared to pure PPY. The dielectric loss spectra ϵ_2 do not reveal any peak as a function of frequency at all temperatures. The experimental dielectric data has been analyzed using electric modulus formalism M^* which is defined as

$$M^*(\omega) = M_1 + iM_2 = \frac{1}{\epsilon^*(\omega)} = \frac{\epsilon_1 + i\epsilon_2}{\epsilon_1^2 + \epsilon_2^2} \quad \textbf{(2)}$$

Isothermal imaginary part of M as a function of frequency for sample S1 are depicted in Fig.8. The spectra exhibit broad peaks at low temperature. The peak frequency shifts to higher frequency with increasing temperature. The relatively larger width and asymmetrical nature of peaks at low temperature suggest the non-Debye behavior of dielectric relaxation process. The shape of M'' peak has been described by Davidson - Cole (DC) function [**32**].

$$M^* = M_\infty[1 - \frac{1}{(1 + i\omega\tau)^\beta}] \quad (3)$$

where τ is the conductivity relaxation time which is given at the frequency of maximum dielectric loss. M_∞ is electric modulus at higher frequency. The parameter β describes the distribution of the relaxation time of the system. Debye relaxation is obtained for $\beta = 1$. The deviation of β from 1 indicates the broad distribution of relaxation time in the spectrum. Fig. 8 shows that the experimental data are reasonably good fitted with the calculated values of DC function. The best fitted parameters are shown in Table II. The values of β are different from unity which imply non- Debye relaxation process at low temperature. Temperature induces Debye process as confirmed form the values of β at $T \geq 175$ K. The relaxation time, τ at different temperatures are determined from the reciprocal of the peak frequency. The Arrhenius plot of ln τ against 1/T for the sample S1 is shown in Fig. 9. A straight-line behavior is obtained. Thus, temperature dependence of relaxation time of loss is given as $\tau \propto \exp(-E/kT)$, E is the activation energy of dielectric process

TABLE I: Weight percentage of pyrrole (x), room temperature dc conductivity (σ(RT)), σ_0, real part of relative dielectric permittivity (ϵ_1) at room temperature (RT)

Sample	x	σ(RT)(10^{-3}) (S/cm)	σ_0(10^3) (S/cm)	ϵ_1(RT)
S4	75	7.51	7.41	3100
S3	68	5.29	12.08	3300
S2	52	3.15	30.94	3500
S1	35	1.95	230.50	3700

and k is Boltzmann constant. The slope of the best fitted straight line gives the activation energy of the sample S1 is 28.4 meV. The value of activation energy for the other two samples S2 and S3 are 43.9 and 48.8 meV respectively. The large dielectric constant is found in other materials such as perovskite oxides [**33**] near the ferroelectric transition and also in high temperature superconductors [34]. The value of ϵ_1 for

polymers are very low compared to inorganic materials. Constant efforts are made to increase this value for more technological applications of polymers. The dielectric constant of polymeric systems can generally be enhanced by adding high dielectric constant particulates. Recently it has been observed that the large dielectric constant can be obtained near the percolation threshold of the composite [35]. Commonly, the mechanism for such enormous value of dielectric constant are Maxwell-Wagner type polarization at the boundary between metallic electrode and the materials. The temperature dependence of dielectric constant at low frequency rules out this possibility in the present composites. The nanocomposite consist of two materials having quite different conductivities and permittivities. The interface across the PPY and CdS may be a source for the large dielectric constant. The dielectric loss spectra ϵ_2 as a function of frequency for S4 are shown in Fig.8 for different temperatures. The relaxation peak in the measured frequency domain is appeared at room temperature. The positions of the peaks move to lower frequency with the decrease of temperature. The dielectric response has been analyzed by the most generalized Havriliak-Negami (HN) function [36]

$$\epsilon^* = \epsilon_\infty + \frac{\epsilon_s - \epsilon_\infty}{(1 + (i\omega\tau)^\beta)^\alpha} \quad (4)$$

where τ is the average relaxation time which is given at the frequency of maximum dielectric loss. The difference $\Delta\epsilon = \epsilon_s - \epsilon_\infty$ is known as the dielectric relaxation strength. The parameter β describes the distribution of the relaxation time of the system. Debye relaxation is obtained for α = 1 and β = 1. The parameters α and β ranging between 0 and 1 are symmetric and asymmetric broadening of dielectric spectra. The solid lines in Fig.8 show that the experimental data are reasonably good fitted with the calculated value of HN function. The value of β is different from unity which implies non- Debye relaxation process. This parameter manifests that the dielectric dispersion has a broad distribution of relaxation time. The dielectric strength Δε increases with increase of temperature.

TABLE II: Davidson-Cole (DC) function best fitted parameters τ and β in Eq. 3 for dielectric loss spectra of sample S1

Temperature (K)	τ(10^{-6}sec)	β
107	5.16	0.932
125	3.34	0.954
150	1.90	0.975
175	1.38	0.999
200	1.11	1
225	0.91	1
250	0.80	1
273	0.75	1
296	0.61	1

The relaxation times, τ at different temperatures are obtained from the best fitted data to eqn.5. The Arrehenius plot (not shown in this manuscript) of ln τ against 1/T for the different samples suggest that the temperature variation of τ can be described by thermally activated Arrhenius law,

$$\tau = \tau_0 exp(E_\tau/kT) \quad (5)$$

where τ_0 is the relaxation time at high temperature, E_τ is the activation energy of dielectric process and k is Boltzmann constant. The slope of the best fitted straight line gives the activation energy as shown in Table II. The most interesting fact is that the activation energies are in excellent agreement with the values obtained from grain conductivity.

IV. CONCLUSION:

The growth and the assemble of CdS nanoparticles in the polymer matrix are a very complicated process. The incorporation of nanosized CdS strongly affects the electronic structure of polypyrrole. The presence of nanocrystalline CdS in the disordered polypyrrole lead to Mott VRH type electric charge conduction.

V. REFERRENCE:

1. Qinglian W, Shi-Zhao K and Jin M, 2004, Physicochem Eng Aspects 247, 125
2. Alivisator A P, 1996, Science, 271, 933
3. Klimov V I, 2006, J Phys Chem B. 110 16827
4. Kolvin V. L, Schlamp M.C and Alivisatos A.P, 1994, Letters to Nature, 370, 354
5. Prasad K. and Jha A.K. Journal of Colloid and Interface Science, 342, 68
6. Hayashi T, Nishikura T, Suzuki T and Ema Y. 1988, J. Appl. Phys. 64(7), 3542
7. Henglein. A, 1989, Chem Rev 89 1861
8. Yang C, Wang L, Zhou Pi Z and Tian X 2009, J. Mater Sci. 44, 3015
9. Pandey Bhawana and Fulekar M. H, 2012, Res. J. Chem. Sci. 2(2), 90
10. Sherman R.L, Chen Y Y and Ford W T, 2004, J. Nanosci. Nanotech 4 1032
11. Nie Q L, Xu Z D, Yuan Q. L and Li G.H, 2003, Mater. Chem. Phys. 82 808
12. Sanghi R. and Verma P. 2009, Chemical Engineering Journal. 155, 886
13. Mathieu H, Richard T, Allegre J, Lefebvre P. and Arnaud G. 1995, J. Appl. Phys. 77, 287
14. Xiong Y, Xie Y, Yang J., Zhang R, Wu C. and Du G, 2002, J. Mater. Chem. 12, 3712
15. Skotheim T. and Elsenbaumer R., 1998, Handbook of Conducting Polymers,Marcel Dekker, New York,
16. Scrosati B, 1993, Application of Electroactive Polymers, Chapman and Hall, London,
17. Epstein A.J, MacDiarmid A.G, 1991, Makromol. Chem., Macromol. Symp. 51, 217
18. Yang Y and Heeger A.J, 1994, Appl. Phys. Lett. 64, 1245
19. Nalwa H. S, Ferroelectric Polymers, Marcel Dekker, New York.
20. Batz P, Schmeisser D and Gopel W. 1991, Phys. Rev. B 43, 9178
21. Bredas J. L, Scott J. C, Yakushi K and Street G. B. 1984, Phys. Rev. B 30, 1023
22. Chang K. J, Froyen S and Cohen M. L 1983, Phys. Rev. B 28 , 4736
23. Nanda J., Kuruvilla B. A. and Sarma D. D. 1999 Phys. Rev. B 59, 7473.
24. Nilen D. W and Hochst H. 1990 Phys. Rev. B 41, 12710
25. Pankove J. I, 1971, Optical Processes in Semiconductors, Prentice Hall, New Jersy,
26. Maxwell J. C. Electricity and Magnetism, (Oxford University Press, England, 1873).vol.1.
27. Wagner K. W, 1913, Annl. Phys. (Leipzig) 40, 53
28. Hippel V., Dielectrics and Waves (Wiley, New York, 1954).
29. Paily R, Dasgupta A, Dasgupta N, Bhattacharya P, Misra P, Ganguli T, Kukreja L. M., Balamurugan A. K., Rajagopalan S. and Tyagi A, Appl. Surf. Sci. 187, 297(2002)
30. Van Dover R. V, 1999, Appl. Phys. Lett. 74, 3041
31. Zuo F, Angelopoulos M, MacDiarmid A. G. and Epstein,A. 1989, J. Phys. Rev. B 39, 3570
32. Davidson D. W. and Cole R. H. 1950, J. Chem. Phys. 18, 1417
33. Lunkenheimer P, Bobnar V, Prinin A V, Ritus A. I., Volkov A and Loidl A. 2002 Phys. Rev. B 66, 052105
34. Cao G and O'Reilly J 1993, J. Crow and L. Testardi, Phys. Rev. B 47, 11510
35. Huang C and Zhang Q. 2003, J. Surf Appl. Phys. Lett. 82 , 3502
36. Havriliak S. and Negami S 1967 Polymer 8, 161